BBA - Molecular Cell Research 1873 (2026) 120087

Contents lists available at ScienceDirect

BBA - Molecular Cell Research

journal homepage: www.elsevier.com/locate/bbamcr

Research paper

Transgenic overexpression of miR-486 and sAnk1.5 does not alter glucose handling in mice

S. Buonocore [a,1,2], F. Fiore [a,1], E.M. Rubino [a,3], M.R. Catallo [a], L. Raucci [a], A. Laurino [a], D. Rossi [a,b], E. Pierantozzi [a,*], V. Sorrentino [a,b,*]

[a] Department of Molecular and Developmental Medicine, University of Siena, 53100, Siena, Italy
[b] Program of Molecular Diagnosis of Rare Genetic Diseases, Azienda Ospedaliera Universitaria Senese, 53100, Siena, Italy

ARTICLE INFO

Keywords:
Skeletal muscle tissue
ANK1 gene internal promoter
sAnk1.5
miR-486
SNP rs508419
T2D susceptibility

ABSTRACT

Recent studies have shown that the C allele of SNP rs508419 is associated with susceptibility to Type 2 diabetes (T2D). This SNP lies within the muscle-specific P2 promoter of human ANK1, which drives transcription of the sAnk1.5 isoform and miR-486. The C allele increases P2 promoter activity, resulting to higher levels of sAnk1.5 transcript and protein in striated muscles.

We now present the first evidence that in skeletal muscle of individuals homozygous for the rs508419 C allele, also the hsa-miR-486-5p is transcribed at higher levels. This raises the question of whether T2D susceptibility may be associated with simultaneous overexpression of miR-486-5p and sAnk1.5. To test this hypothesis, we generated and characterized double transgenic (D-Tg) mice that selectively overexpress both mmu-miR-486-5p and sAnk1.5 in skeletal muscle tissue.

Analysis of sAnk1.5 and miR-486-5p expression in D-Tg mouse showed that despite both transgenes were significantly upregulated, a discrepancy between sAnk1.5 mRNA and protein levels was observed, suggesting that sAnk1.5 protein levels are further regulated by post-translational mechanism. D-Tg mice were monitored from 2 to 12 months of age to assess body weight, fat and lean mass, blood glucose levels under fasting conditions, as well as during intraperitoneal glucose tolerance tests and insulin tolerance tests, performed under either standard or high fat diet conditions. No differences were observed between D-Tg and age-matched wild type control mice for any of the parameters tested, indicating that the link between rs508419 and susceptibility to T2D cannot be ascribed to increased expression of miR-486-5p and sAnk1.5 in skeletal muscle.

1. Introduction

The *ANK1* gene encodes ankyrin-1 (also known as ankyrin-R), a large cytoskeletal protein initially identified in erythrocytes as a spectrin-binding protein, and thus essential for maintaining the biconcave shape of red blood cells and stabilizing the plasma membrane against mechanical stress. Beyond erythrocytes, ankyrin-1 is also expressed in several other tissues, including neurons and striated muscles, where it similarly plays a critical role in maintaining cellular integrity by anchoring integral membrane proteins to the spectrin–actin cytoskeleton. The canonical full-length ankyrin-1 protein (206 kDa) has a structure that consists of three major domains: 1) a membrane-binding domain (containing ankyrin repeats); 2) a spectrin-binding domain; and 3) a C-terminal regulatory domain, often referred to as a death domain. Alternative splicing events and post-translational modifications further diversify the types of protein present both within the same cell type and across different tissues, generating a variety of ankyrin-1 isoforms that typically range in size from 170 to 210 kDa [1,2]. These large isoforms of ANK1 are encoded by mRNAs transcribed from the *ANK1* main promoter (P1), located in the 5′ region of the gene [3]. In addition to these large isoforms, a non-canonical, muscle-specific ankyrin-1 isoform, with a lower molecular weight, has been identified in striated muscle tissues [3–5]. This small isoform, called sAnk1.5, is encoded by a mRNA transcribed from an internal promoter (P2), active only in

* Corresponding authors at: Department of Molecular and Developmental Medicine, University of Siena, Via Aldo Moro 2, 53100, Siena, Italy.
E-mail addresses: enrico.pierantozzi@unisi.it (E. Pierantozzi), vincenzo.sorrentino@unisi.it (V. Sorrentino).
[1] These authors contributed equally to this work.
[2] Buonocore S, present address: Department of Biology, University Federico II, Naples, Italy.
[3] Rubino EM, present address: Department of Pharmacy-Drug Sciences, University of Bari "Aldo Moro", Bari, Italy.

https://doi.org/10.1016/j.bbamcr.2025.120087
Received 11 July 2025; Received in revised form 6 November 2025; Accepted 13 November 2025
Available online 17 November 2025

striated muscle tissue and located in the 3′ region of the *ANK1* gene [4–7].

sAnk1.5 protein has a molecular weight of approximately 17 kDa and is structurally distinct from full-length ankyrin-1. Notably, it lacks both the membrane-binding and spectrin-binding domains but it contains, in its N-terminal region, 22 additional amino acids that form a hydrophobic transmembrane helix that anchors the protein to the sarcoplasmic reticulum (SR) membrane of striated muscle cells [5–7]. The C-terminal region of sAnk1.5 extends into the cytoplasm and interacts with the COOH terminus of obscurin, a giant sarcomeric protein [8–11]. A number of studies have clearly shown that the interaction between sAnk1.5 and obscurin establishes a link that stabilizes the SR around the myofibrils [11–18]. Indeed, sAnk1.5 knockout (KO) mice exhibit a reduction in SR volume and altered Ca^{2+} homeostasis, a biological process essential for regulating physiological muscle function and frequently altered in muscle diseases [18–21]. In addition, recent evidence suggests a potential role for sAnk1.5 in regulating the activity of the sarco(endo)plasmic reticulum Ca^{2+}-ATPase 1 (SERCA1). This regulatory function has been proposed to be mediated by the transmembrane domain of sAnk1.5 that shares sequence homology with known regulators of SERCA, such as sarcolipin (SLN) and phospholamban (PLN) [22–24].

Through Genome-Wide Association Studies, genome-mapping, trait–gene- and Type 2 Diabetes- (T2D) expression association, two independent groups identified a novel single nucleotide polymorphism (SNP), rs508419, located within the P2 promoter of the *ANK1* gene [25,26], whose C allele has been linked to increased susceptibility to T2D [25–30]. Importantly, differential expression analyses, cis-eQTL mapping, luciferase assays, and electrophoretic mobility shift assays indicated that the presence of the C allele enhanced the activity of the *ANK1* P2 promoter, resulting in increased levels of sAnk1.5 in skeletal muscles [25,26]. To investigate a potential link between elevated sAnk1.5 protein levels and T2D susceptibility, we previously generated a transgenic mouse model selectively overexpressing sAnk1.5 in striated muscles ($Tg^{sAnk1.5}$). However, characterization of $Tg^{sAnk1.5}$ mice showed that sAnk1.5 overexpression had no effect on glucose handling or other parameters commonly altered in pre-diabetic or diabetic conditions [31]. Additionally, analysis of the *ANK1* gene sequence revealed the presence of a microRNA, miR-486, in intron 42 of the *ANK1* gene [ENSG00000029534] [32]. MiR-486, whose mature forms, namely miR-486-5p and miR-486-3p, exhibit complete (100 %) sequence identity between humans and mouse (miRBASE, http://mirbase.org/, Accession: MI0002470 and MIMAT0003130, respectively), can be transcribed by the P1 and P2 promoters of the *ANK1* gene, resulting in its selective enrichment in striated muscle tissue [32–34]. Interestingly, among the potential targets of miR-486-5p, which, both in humans and mice, has been studied much more extensively compared to miR-486-3p, there are mRNAs coding for proteins involved in glucose regulation; these include PTEN, FOXO1, and DOCK3, whose inhibition may enhance the activity of the AKT pathway. Notably, these validated targets of miR-486-5p harbor, in both humans and mice, an identical sequence corresponding to the miR-486-5p seed region [32,34–38]. On the other hand, other evidence suggests that miR-486-5p might also target the mRNAs of IGF1, IGF1R and the p85α regulatory subunit of phosphoinositide-3-kinase (PIK3R1), thus resulting in the downregulation of the AKT pathway [37–40]. Nevertheless, functional studies in mice have shown that miR-486-5p exerts a trophic effect in skeletal muscle tissue, by promoting fiber regeneration and regulating fiber size. Accordingly, miR-486-5p may also contribute to limit sarcopenia- and cachexia-dependent muscle loss [37,41]. In addition, miR-486-5p overexpression is also able to reverse skeletal muscle defects observed in mouse models of Duchenne Muscle Dystrophy and cancer [34,37–43].

Based on evidence that miR-486 is generated by the muscle-specific P2 promoter, and that the C allele of rs508419 enhances the transcriptional activity of the P2 promoter, we investigated whether miR-486-expression was increased in skeletal muscle biopsies from individuals carrying the C allele. Our analysis revealed that, in skeletal muscle, the levels of hsa-miR-486-5p are expressed several hundred-fold higher than those of hsa-miR-486-3p. In addition, we observed that, in individuals homozygous for the rs508419 C allele, hsa-miR-486-5p levels are 3-fold higher than those observed in individuals homozygous for the T allele. On this basis, we hypothesized that the rs508419 SNP might predispose to T2D susceptibility by enhancing the expression of both miR-486-5p and sAnk1.5. To verify this hypothesis, we generated a double transgenic (D-Tg) mouse model selectively overexpressing miR-486 and sAnk1.5 in skeletal muscle. We assessed body weight, fat and lean mass, and blood glucose levels under fasting conditions, as well as during intraperitoneal glucose tolerance tests (IPGTT) and insulin tolerance tests (IPITT) in D-Tg mice under either standard or high fat diet conditions. No differences were observed between D-Tg and control mice for any of the parameters tested.

The results reported indicate that the link between rs508419 and susceptibility to T2D cannot be explained by increased expression of miR-486-5p and sAnk1.5 in skeletal muscle.

2. Methods

2.1. Human skeletal muscle biopsies

This study complies with the ethical standards laid down in the 1964 Declaration of Helsinki. The skeletal muscle biopsies from *vastus lateralis* used in this study were collected between 2014 and 2019 (Supplementary Table 1) during routine diagnostic procedures, after obtaining informed consent from all patients. The use of the biopsies for scientific purposes was approved by the Regional Ethics Committee for Clinical Trials of the Tuscany Region (Protocol No. 16342). All biopsies, anonymized immediately upon collection, were snap frozen in liquid nitrogen and immediately stored at −80 °C for extraction of DNA, RNA, or total proteins. To define the SNP genotype of single individuals, genomic DNA was extracted with the Gentra Purgene kit (Qiagen, Hilden, Germany) according to manufacturer's instructions. The genomic region containing the rs508419 in *ANK1* (NC_000008.10) was amplified by PCR (T-100 Thermal Cycler, BioRad, Hercules, California, USA), using the following pair of primers: hSNP FW: 5'–GCCCATCACTCACCCTTTTG–3′ and hSNP REV: 5′–AGCTGGTTTGGGGAGGTAAA–3′ (Sigma-Aldrich, St. Louis, MO, USA). Amplified DNA was sequenced by PCR-based standard capillary Sanger sequencing as previously described (Applied Biosystems 3500 Series Genetic Analyzer) [44]. The sequences obtained were analyzed by SnapGene software, version 8.1 (GSL Biotech LLC, Chicago, IL, USA).

2.2. Mice

All the procedures were conducted to ensure minimal animal distress, and were approved by the Animal Care Committee of the University of Siena (OBPA, 7DF19.27 and 7DF19.28), and finally authorized by the Italian Ministry of Health (N. 27_2020-PR and N. 29_2020-PR). All experimental protocols adhered to the European Parliament and Council Directive 2010/63/EU concerning the protection of animals used for scientific research, and the study complies with the ARRIVE guidelines (https://arriveguidelines.org). Experiments were carried out using adult male C57BL/6J mice aged between 2 and 12 months. Animals were provided with unrestricted access to food and water and housed under controlled conditions with temperatures maintained between 21 and 25 °C, relative humidity of 50–60 %, and a 12-hour light/dark cycle. D-Tg mice ($Tg^{sAnk1.5}/Tg^{miR486}$) were generated by crossing the C57BL/6-Tg(p-Mex-MLC-sAnk1.5) [31] with the C57BL/6J-Tg(Ckm-Mir486)2Lmk/J line (purchased from The Jackson Laboratory, JAX stock #030449) [40]. Both founder mouse lines are viable and fertile; mir-486 overexpressing mice show no significant physical or behavioral differences from non-carrier mice, except for a modest increase in body weight [31,40]. D-Tg mice were fertile, were born at the expected Mendelian ratio, and presented an

indistinguishable phenotype from wild type (WT) sibling mice. Weanlings were genotyped by PCR as previously described [31,40]. For high fat diet (HFD) treatment, 2-month-old WT and D-Tg male mice were randomly allocated into four experimental groups: WT and D-Tg control groups received a standard chow diet, whereas WT and D-Tg treated groups were fed a HFD containing 45 % of metabolizable energy from fats for 12 weeks (PF1916, Mucedola s.r.l., Italy). Mice anesthetized with 2 % isoflurane were euthanized by cervical dislocation.

2.3. Quantitative analysis of sAnk1.5 and miR-486

Total RNA was extracted from mouse tissues and human skeletal muscle biopsies as described in [31,45], respectively. RT-qPCR on human (H) and mouse (Ms) sAnk1.5 cDNA was performed as described in [46], using the following pair of primers: H-sAnk1.5 fw: 5′CTGGTGCTGTTAGGCTTCTTC 3′, H-sAnk1.5 rev: 5′ GTTCCTGGTGGATGTGCTTC 3′; H-β-Actin fw: 5′ CAACTCCATCATGAAGTGTGAC 3′; H-β-Actin rev: 5′ GCCATGCCAATCTCATCTTG 3′; Ms-sAnk1.5 fw: 5′ GAGGAGATCCTTCTTTTGTTCCA 3′, Ms-sAnk1.5 Rev.: 5′ GGACGTGGT GACCCACCTG 3′; Ms-GAPDH fw: 5′ CCAGAATGGGAAGCTTGTC 3′, Ms-GAPDH rev: 5′ TCTCGCTCCTGGAAGATGGT 3′. miR-486 cDNA was prepared using the TaqMan MicroRNA Reverse Transcription Kit, and RT-qPCR was carried out on a QuantStudio 5 real-time PCR system (Applied Biosystems), using the TaqMan MicroRNA Assay validated for human and mouse miR-486-5p and -3p (assay ID: 001278 and 002093, respectively; Thermo Fisher Scientific, Waltham, MA, USA), following manufacturer's protocol. Relative expression levels of both targets were calculated by the ΔΔCt method [47], using human β-Actin, mouse GAPDH and U6 small nuclear RNA (assay ID:001973, U6 snRNA) as endogenous controls, and sAnk1.5 and miR-486 expression levels in human T/T samples and WT mice as reference samples.

2.4. SDS-page and immunoblot

Total proteins lysates were prepared, quantified, separated and transferred onto a nitrocellulose membrane as in [48]. Briefly, skeletal muscles were homogenized in RIPA buffer (Cell Signaling Technology) supplemented with 1 mM (phenylmethylsulfonyl fluoride, Sigma-Aldrich), and total protein content was quantified using the Pierce Protein Assay/bicinchoninic acid assay (Thermo Fisher Scientific). 40 μg of total proteins were separated on 4–20 % SDS-PAGE (Novex, Invitrogen by Thermo Fischer Scientific) and transferred onto a nitrocellulose membrane using the Trans-Blot Turbo Transfer System (Bio-Rad). Membranes were stained with Ponceau S (Thermo Fisher Scientific), blocked with working solution (WS: 5 % low fat milk or BSA in 20 mM Tris–HCl pH 7.4, 150 mM NaCl, and 0.1 % Tween 20) for 1 h at room temperature, and then incubated overnight at 4 °C with the following primary antibodies, all diluted 1:1000 in WS: custom polyclonal rabbit anti-sAnk1.5 [13]; polyclonal rabbit anti-AKT(pan) (C67E7), polyclonal rabbit anti-phospho-AKT (Ser473) (193H12), polyclonal rabbit anti phospho-AKT (Thr308) (C31E5E), polyclonal rabbit anti-PTEN (138G6), polyclonal rabbit anti-FoxO1 (C29H4) (all from Cell Signaling Technology). Membranes were incubated for 1 h at room temperature, with HRP-conjugated secondary antibody (Cell Signaling Technology) diluted 1:2500 in WS. For total AKT analysis, the membranes incubated with anti-phospho-AKT were stripped at 56 °C for 20 min in 10 ml of stripping solution (2 % SDS, 0.062 M Tris–HCl pH 6.8, 0.8 % 2-mercaptoethanol) (Sigma-Aldrich, St Louis, MO). To detect HRP signal, membranes were incubated with Enhanced Chemi-Luminescence solutions (Bio-Rad, Hercules, CA, USA) for 5 min and the luminescent signal was acquired by ChemiDoc luminescence counter (Bio-Rad, Hercules, CA, USA). Quantification of the intensities of immunoreactive bands was performed by Image Lab software version 6.1 (BioRad, Hercules, CA, USA).

2.5. Immunofluorescence on isolated fibers

Flexor digitorum brevis (FDB) muscles excised from 2-month-old WT and D-Tg mice were prepared as previously described [49]. In brief, single fibers were mechanically isolated from excised FDB muscles, laid on laminin-coated coverslips, and fixed in 1 % PFA/0.5 % Triton X-100 solution (all from Sigma-Aldrich, St Louis, MO, USA). Monoclonal antibody against α-actinin (clone EA-53, Sigma-Aldrich; dilution: 1:1000) was used to identify the *Z*-disks, and custom polyclonal rabbit anti-sAnk1.5 (dilution: 1:500) [13] was used to immunolocalize sAnk1.5. Cy3-conjugated anti-rabbit IgG (Jackson ImmunoResearch, UK) or Alexa Fluor488-conjugated anti-mouse IgG secondary antibodies (Thermo Fisher Scientific), both diluted 1:1000, were used to reveal target proteins. Fibers were imaged and acquired as in [50].

2.6. MG-132 treatment

100 μl of 20 μM MG-132 (M7449, Sigma-Aldrich) were injected in the gastrocnemius muscle of 6 months-old male mice. Contralateral muscle was injected with 100 μl of PBS containing 0.2 μl of DMSO. Mice were sacrificed 24 h after injection, and gastrocnemius muscles were excised and processed to obtain total protein lysates.

2.7. Intraperitoneal glucose and insulin tolerance tests

Glucose tolerance tests were conducted on male mice aged 2, 6, 10, and 12 months that were fed a standard chow diet, as well as on 5 months-old mice following a 12-week high-fat diet. Prior to testing, mice underwent an overnight fast and were weighed. Each mouse received an intraperitoneal injection of 20 % D-glucose solution (Sigma-Aldrich) at a dose of 10 μl per gram of body weight, equivalent to 2 g/kg glucose. Insulin tolerance tests were carried out on 6 and 12 months-old male mice. After a 5-h morning fast (8 a.m. to 1 p.m.), animals were weighed, and insulin solution (100 U/ml, diluted 1:1000; Eli Lilly Italia S.p.A.) was administered intraperitoneally at 10 μl per gram of body weight, corresponding to a dose of 1 U/kg. Blood glucose concentrations were monitored by collecting a drop of blood from the tail tip and applying it to a glucometer strip (OGC care, Biochemical System International, Arezzo, Italy). Measurements were taken before injection (time 0), at 30- 60- 120- and 180-minutes post-glucose injection, and at 15- 30- 60- 90- and 150-minutes following insulin administration. Serum insulin concentrations were quantified using a mouse insulin ELISA kit, according to the manufacturer's protocol, with mouse insulin as the calibration standard (Mercodia, Uppsala, Sweden).

2.8. Statistical analysis

Results are presented as mean values ± standard deviation (SD). Differences between groups for each measured variable were evaluated using an unpaired Student's *t*-test. The areas under the curve (AUC) from glucose and insulin tolerance tests were analyzed by two-way ANOVA, followed by Bonferroni's multiple comparisons test. The F-test was applied to assess significance, with *p*-values below 0.05 deemed statistically significant. All analyses were conducted using GraphPad Prism software version 10.4.1.

3. Results

3.1. Effect of rs508419 genotype on expression of miR-486 and sAnk1.5

Analysis of the rs508419 genotype of 260 Caucasian individuals revealed that the rs508419 C/C, C/T, and T/T genotypes were present at a frequency of 53 % ($n = 137$), 40 % ($n = 105$), and 7 % ($n = 18$),

respectively. These findings are consistent with previous reports [25,26] and with data available in public databases (NCBI SNP database, National Institutes of Health, https://www.ncbi.nlm.nih.gov/snp/rs508419#frequency_tab).

To evaluate the impact of the rs508419 genotype on miR-486 expression, qPCR analysis was performed on total RNA extracted from skeletal muscle biopsies of 15 individuals homozygous for the T allele (genotype T/T) and from 14 individuals homozygous for the C allele (genotype C/C) of SNP rs508419 (Supplementary Table 1). As shown in Supplementary Fig. 1A–C, we observed that hsa-miR-486-5p is the predominant mature isoform, expressed several hundred-fold higher than hsa-miR-486-3p. As reported in Fig. 1A, hsa-miR-486-5p expression levels were nearly 3-fold higher in skeletal muscle biopsies from individuals homozygous for the C allele compared to those homozygous for the T allele. No change in the hsa-miR-486-3p levels was observed in skeletal muscle from individuals carrying either the C/C or T/T genotype (Supplementary Fig. 1D). In parallel experiments, mRNA and protein expression levels of sAnk1.5 were measured in available biopsies. The results demonstrated that sAnk1.5 mRNA and protein levels were increased by approximately three and two folds, respectively, in individuals carrying the C/C genotype compared to those with the T/T genotype (Fig. 1B–D and Supplementary Fig. 1E, F), consistent with previously reported data [25,26].

3.2. miR-486-5p and sAnk1.5 expression pattern in $Tg^{sAnk1.5/miR-486}$ double transgenic mice

The novel finding that the rs508419 C/C genotype is also associated with an increase in hsa-miR-486-5p expression in skeletal muscle, prompted us to investigate whether the concurrent overexpression of sAnk1.5 and miR-486-5p might associate with T2D susceptibility. To verify this, we crossed transgenic mice overexpressing sAnk1.5 [31] and mmu-miR-486-5p [34,38] to generate a double transgenic mouse line (D-Tg) in which sAnk1.5 and mmu-miR-486-5p were simultaneously overexpressed in skeletal muscle. Skeletal muscle–specific overexpression of sAnk1.5 and mmu-miR-486-5p was confirmed in skeletal muscle tissue using both Western blot and real-time PCR (Fig. 2A–C and Supplementary Fig. 2A–C). In addition, immunofluorescence experiments revealed that, in skeletal muscle fibers of D-Tg mice, sAnk1.5 localized to the M-band and *Z*-disk of the sarcomere (Supplementary Fig. 2D), a pattern consistent with the localization of endogenous sAnk1.5 in wild-type muscle fibers [11–13].

Quantitative analysis of sAnk1.5 expression in the skeletal muscle of D-Tg mice revealed a discrepancy between the relative abundance of sAnk1.5 mRNA and its corresponding protein. This discrepancy, previously observed in two different mouse lines, $Tg^{sAnk1.5}$ and obscurin KO mice [15,31], likely reflects a post-translational regulation of sAnk1.5 protein expression. Indeed, it has been proposed that ubiquitin and/or ubiquitin-like modifiers may mediate sAnk1.5 degradation via the proteasome [15,51]. Supporting this hypothesis, intramuscular administration of the proteasome inhibitor MG132 in D-Tg mice led to a significant increase of ~35 % of sAnk1.5 protein levels compared to untreated contralateral muscles (Supplementary Fig. 3A, B). In addition, a noticeable increase in the sAnk1.5 "laddering effect", a pattern indicative of ubiquitin-dependent post-translational modifications [52], was also observed (Supplementary Fig. 3C, D).

On the other hand, quantification of mmu-miR-486-5p expression in skeletal muscles of D-Tg mice mirrored the results previously reported for the Tg-Ckm-Mir486 mouse line (Fig. 2C; [38]). Accordingly, overexpression of miR-486 in D-Tg skeletal muscles resulted in a significant reduction of expression of both PTEN and FoxO1 (Supplementary Fig. 4A–D), two validated targets of this microRNA both in humans and mice [32,34,38].

3.3. Body weight, fat and muscle mass of D-Tg mice

Randomly selected WT and D-Tg mice (n = 13 and 15, respectively) were monitored over a twelve-month period by recording body weight at 2, 6, 10, and 12 months of age. As shown in Fig. 3A, no differences in body weight were observed between WT and D-Tg mice at any time point. Additionally, body fat and muscle mass were quantified in 10-month-old WT and D-Tg mice (n = 5 per group). Adipose tissue included cervical, intrascapular, axilla-thoracic, mesenteric, abdominal-pelvic, retroperitoneal, epididymal, and inguinal fat pads (Fig. 3B), while skeletal muscles included extensor digitorum longus (EDL), soleus, tibialis anterior (TA), and gastrocnemius. As shown in Fig. 3C–G, no significant differences were observed between WT and D-Tg mice in either fat mass (WT = 2.17 ± 0.68 g; D-Tg = 1.79 ± 0.74 g) or skeletal muscle mass (EDL WT = 11.99 mg ± 1.39 and EDL D-Tg =12.32 ± 1.15; Soleus WT = 11.13 mg ± 0.88 and Soleus D-Tg =10.89 ± 0.81; TA WT

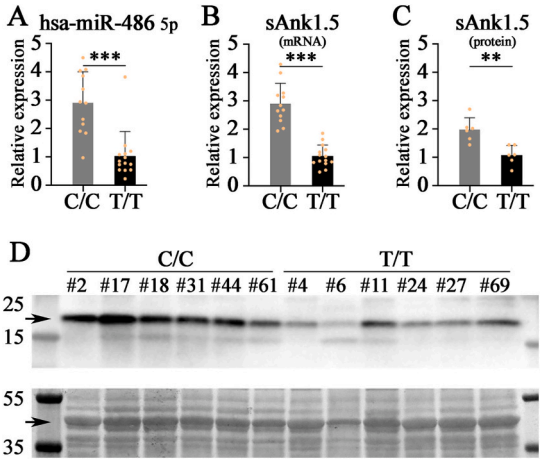

Fig. 1. Expression of hsa-miR-486-5p and sAnk1.5 in skeletal muscle biopsies from individuals carrying the C/C and the T/T genotypes. Quantification of hsa-miR-486-5p (A) and sAnk1.5 mRNA (B) expression levels in total RNA extracted from muscle biopsies of 12C/C and 14 T/T healthy individuals. C. Densitometric analysis of sAnk1.5 band intensity obtained from western blot in total lysates prepared from muscle biopsies of individuals carrying either C/C or T/T genotypes (D). Arrow in the upper panel points to sAnk1.5 signal; arrow in the lower panel (Ponceau-Red staining) points to actin that was used as normalizer for densitometric analysis. # identifies the tag number of single individuals. Hsa-miR-486-5p and sAnk1.5 expression levels are reported as fold change ± sd relative to T/T that was set as 1. ** = $p < 0.01$, *** = $p < 0.001$ as calculated by Student's *t*-test. (For interpretation of the references to color in this figure legend, the reader is referred to the web version of this article.)

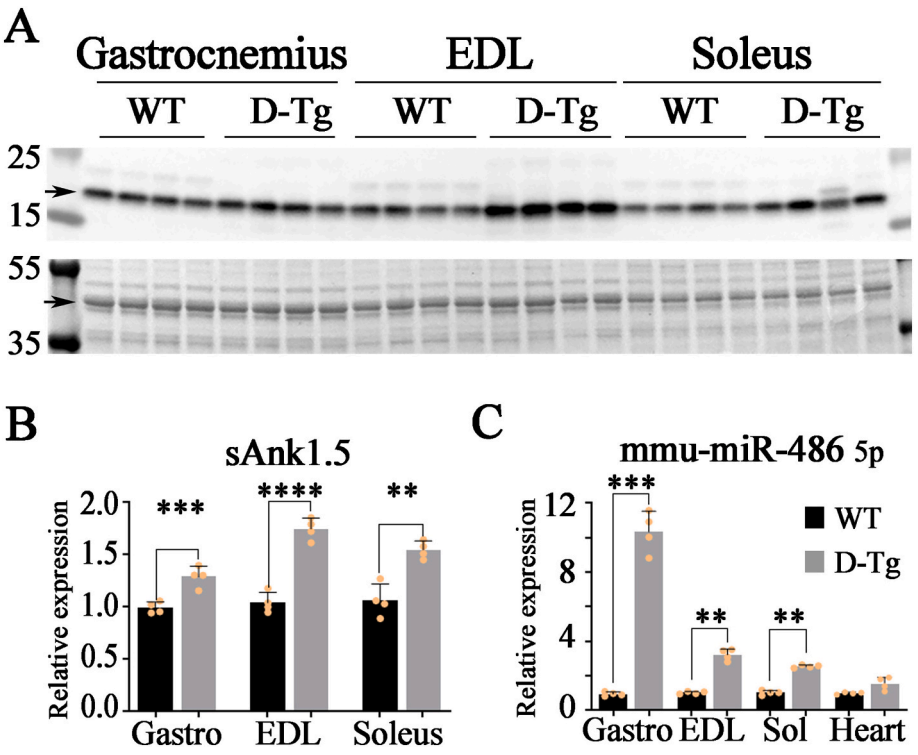

Fig. 2. sAnk1.5 and mmu-miR-486-5p expression pattern in skeletal muscles of D-Tg mice. A. Western blot analysis of sAnk1.5 (arrow in the upper panel) in total lysates prepared from gastrocnemius, EDL and soleus muscles excised from 6-month-old WT and D-Tg mice ($n = 4$ for both mouse lines). B. Densitometric analysis of sAnk1.5 band intensity using actin (arrow in the Ponceau-Red image reported in the lower panel of A) as normalizer. C. Quantification of mmu-miR-486-5p expression levels in total RNA extracted from striated muscles excised from 6-month-old WT and D-Tg mice (n = 4 for both mouse lines). sAnk1.5 and mmu-miR-486-5p expression levels are reported as fold change ± sd relative to WT muscles that were set as 1. ** = $p < 0.01$, *** = $p < 0.001$, **** = $p < 0.0001$ as calculated by Student's *t*-test. (For interpretation of the references to color in this figure legend, the reader is referred to the web version of this article.)

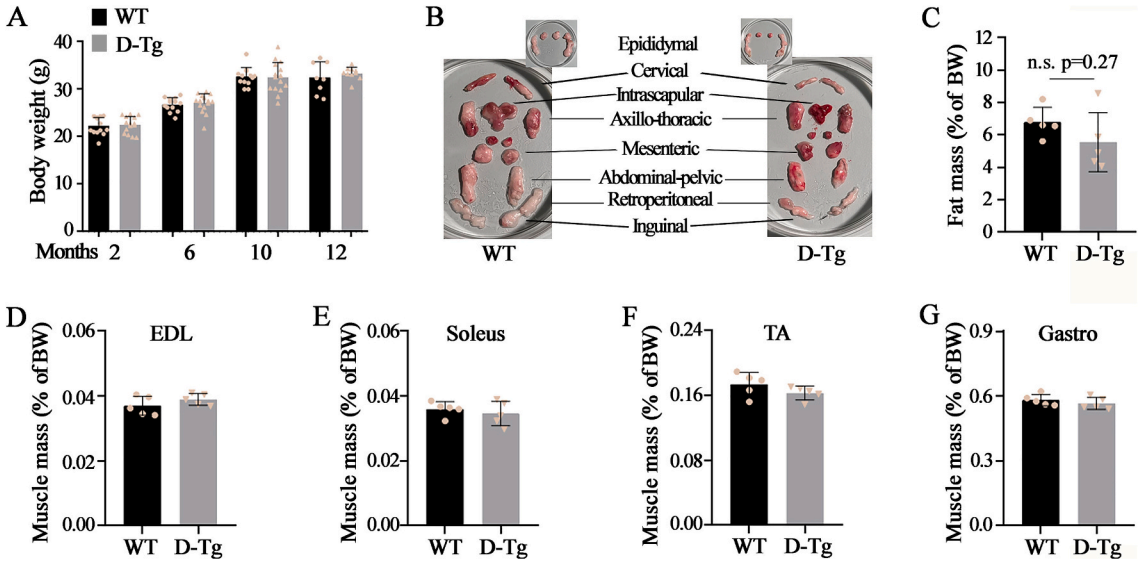

Fig. 3. Body weight, fat and lean mass of D-Tg mice. A. Body weight (grams ± sd) of WT and D-Tg mice at 2, 6, 10 and 12 months of age. B. Anatomical regions of adipose tissue sampling. C. Body fat mass of 10-months-old WT and D-Tg mice, calculated from the sum of the weight of the adipose depots indicated in B, and reported as percentage ± sd of total body weight. n.s. = not significant. EDL (D), soleus (E), tibialis anterior (TA) (F) and gastrocnemius (gastro) (G) mass of 10-months-old male WT and D-Tg mice reported as percentage ± sd of total body weight (BW).

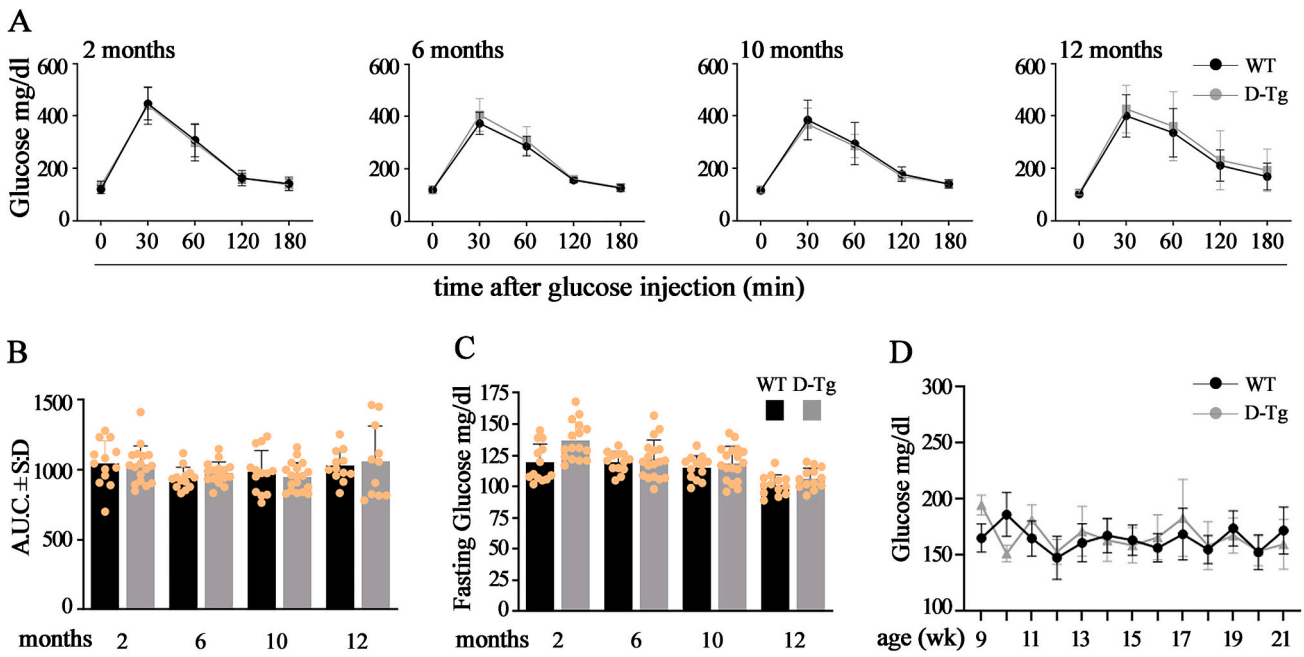

Fig. 4. Glycemic phenotype of D-Tg mice. A. Glycemic curves of WT and D-Tg mice obtained during glucose tolerance tests (IPGTT) performed at 2, 6, 10, and 12 months of age. n = 13 WT and 15 D-Tg mice at 2, 6 and 10 months of age; n = 8 WT and 10 D-Tg mice at 12 months of age. B. Area under the curve (A.U.C.) calculated from the glycemic curves shown in A. C. Blood glucose levels of WT and D-Tg following 17 h of fasting. D. Weekly monitoring of baseline blood glucose of WT and D-Tg mice between 9 and 21 weeks of age. All values are presented as the mean ± sd.

= 52.12 mg ± 5.42 and TA D-Tg =51.54 ± 3.72; Gastrocnemius WT = 175.51 mg ± 6.19 and Gastrocnemius D-Tg =179.10 ± 16.59).

3.4. Blood glucose analysis in D-Tg mice under standard chow diet condition

To evaluate whether skeletal muscle–specific overexpression of both sAnk1.5 and miR-486-5p is associated with T2D susceptibility, the glycemic profile of D-Tg mice fed a standard chow diet was monitored over 12 months. Fasting glucose levels at 2, 6, 10, and 12 months of age were comparable between D-Tg mice and age-matched WT controls (Fig. 4A, C). Additionally, basal blood glucose levels recorded weekly over twelve consecutive weeks, from 2 to 6 months of age, a period spanning the transition from young to mature adulthood, were similar in both experimental groups (Fig. 4D). Importantly, glycemic curves following intraperitoneal administration of glucose (2 g/kg) were nearly identical between WT and D-Tg mice at 2, 6, 10, and 12 months of age (Fig. 4A, B). Accordingly, overall glucose tolerance, assessed by the area under the curve (AUC) of the glycemic responses, was similar between WT and D-Tg mice at each time point analyzed (Fig. 4B).

Taken together, these results indicate that overexpression of sAnk1.5 and miR-486-5p does not affect glucose handling in skeletal muscle.

3.5. Insulin response in D-Tg mice under standard chow diet condition

To exclude the possibility that the unaltered glycemic response following glucose injection was due to increased insulin release in D-Tg mice, serum insulin levels during the intraperitoneal glucose tolerance test (IPGTT, Fig. 4A) were evaluated in 10-month-old WT and D-Tg mice, both after overnight fasting and post-glucose injection. As shown in Fig. 5A, circulating insulin levels were comparable between the two groups after 17 h of fasting. Similarly, 30 and 120 min after glucose administration, the increase in circulating insulin was comparable between WT and D-Tg mice, indicating that D-Tg mice modulate insulin release as efficiently as WT controls.

Consistent with these findings, intraperitoneal insulin tolerance tests (IPITT) revealed no differences between 6- and 12-month-old D-Tg mice and age-matched WT mice (Fig. 5B, C), further indicating that insulin sensitivity is not altered in D-Tg mice.

Furthermore, analysis of AKT activation following insulin stimulation, a pathway often impaired in (pre)diabetic mouse models [53], showed that the levels of phosphorylated AKT at both Ser473 and Thr308 residues in skeletal muscle of D-Tg mice were similar to those observed in WT mice (Fig. 5D–G).

3.6. Blood glucose analysis in D-Tg mice under high-fat diet condition

Since susceptibility to T2D may not manifest solely with aging, a high-fat diet (HFD) providing 45 % of energy from fats is commonly used to induce obesity. This treatment increases fat mass, impairs glucose tolerance, and accelerates insulin resistance in susceptible mice [54,55]. To further investigate the association between skeletal muscle–specific overexpression of miR-486-5p and sAnk1.5 and T2D susceptibility, 2-months-old WT and D-Tg mice were fed an HFD for twelve weeks. Control groups for both genotypes were simultaneously maintained on a standard diet (chow). Consistent with prior findings, glucose tolerance was comparable between WT and D-Tg mice before the HFD protocol (Fig. 6A). As expected, glucose and insulin tolerance deteriorated in all HFD-fed mice compared to chow-fed controls (Fig. 6B, C). However, even after HFD treatment, glucose and insulin tolerance of D-Tg mice did not differ from those of WT mice (Fig. 6B, C insets). Additionally, after twelve weeks on HFD, weight gain, body fat, and muscle mass of D-Tg mice were not significantly different from those of WT diet-matched controls (Fig. 6D–G, Table 1 and Supplementary Fig. 5A, B). These results indicate that overexpression of miR-486-5p and sAnk1.5 in skeletal muscle does not alter the metabolic response to HFD, with D-Tg mice exhibiting responses comparable to WT.

4. Discussion

The main aim of the present study was to investigate the potential mechanisms at the basis of the reported association between the C/C genotype of the SNP rs508419, located in the striated muscle-specific ANK1 P2 promoter, and T2D susceptibility. Our interest was initially

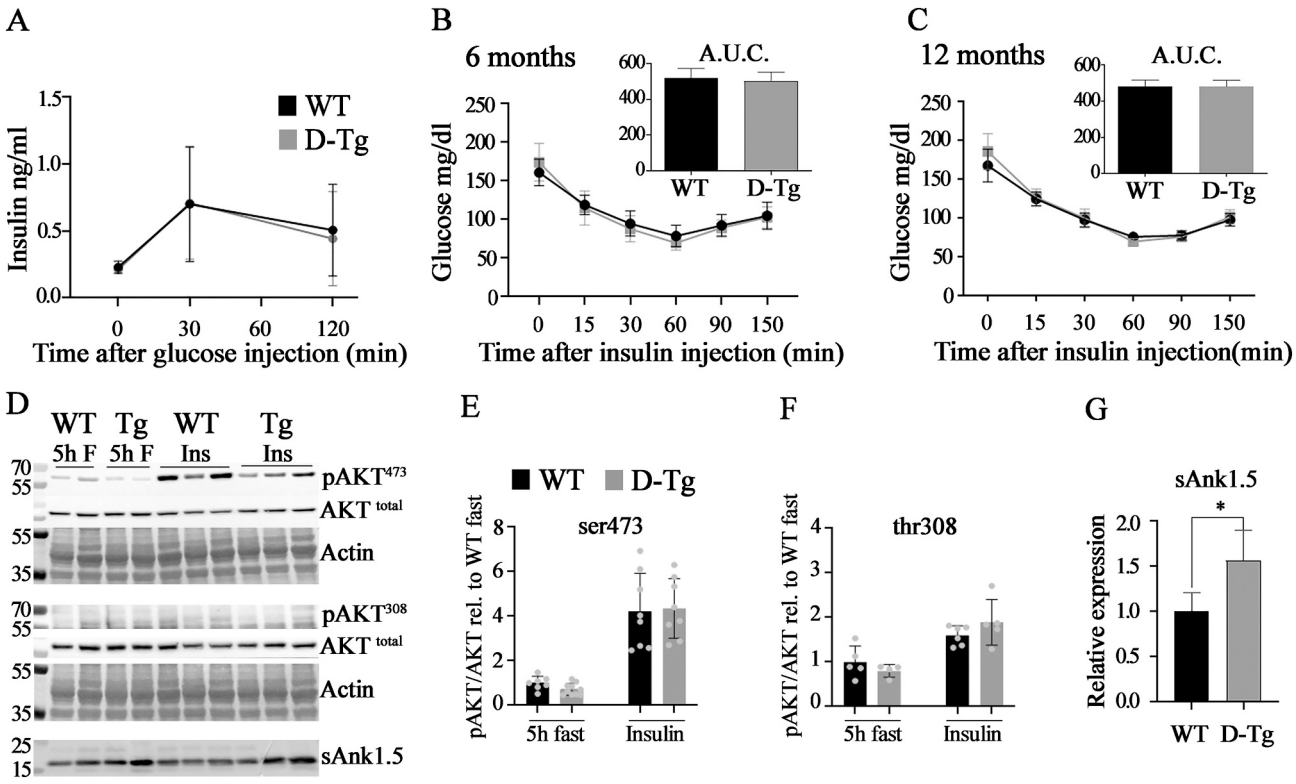

Fig. 5. Insulin response in D-Tg mice. A. Blood insulin levels (ng/ml) of 6 months-old WT and D-Tg mice following 17 h of fasting (t0) and 30 and 120 min after glucose injection (t30, t120). Glycemic curves of WT and D-Tg mice obtained during the insulin tolerance tests (IPITT) performed at 6 (B) and 12 (C) months of age. Insets: Area Under the Curve (A.U.C.) calculated from the glycemic curves. n = 13 WT and 13 D-Tg mice. D. Representative western blot analysis for phosphorylated AKT at serine 473 ($pAKT^{473}$) and threonine 308 ($pAKT^{308}$), total AKT (AKT^{total}) and sAnk1.5 on whole lysates prepared from the gastrocnemius muscle of 7 months-old WT and D-Tg mice either fasted for 5 h (lanes 1–4), and after 15 min following insulin injection (lanes 5–10). Ponceau-red staining of actin is reported as loading control. Densitometric analysis of $pAKT^{473}$ (E), $pAKT^{308}$ (F) and sAnk1.5 (G) immunoreactive bands. The expression levels of phosphorylated AKT are reported as fold change of the mean ± sd of the ratio between pAKT and total AKT compared to WT fasted muscles. The expression levels of sAnk1.5 are reported as fold change compared to WT muscles. * = $p < 0.05$ as calculated by Student's *t*-test. (For interpretation of the references to color in this figure legend, the reader is referred to the web version of this article.)

stimulated by previously published data indicating that the C/C genotype increased the P2 promoter activity resulting in higher levels of sAnk1.5 expression [25,26]. However, transgenic mice overexpressing sAnk1.5 did not result in alteration in glucose homeostasis [31]. On the other hand, additional evidence revealed that the P2 promoter also regulates the expression of miR-486 [32,39,56]. We thus investigated whether, the C/C genotype of rs508419 could also alter the expression of miR-486. We report here evidence that skeletal muscles from individuals carrying the C/C genotype express higher levels of hsa-miR-486-5p compared to individuals with the T/T genotype, similarly to what observed for sAnk1.5 (25, 26). Furthermore, we demonstrated that, in human skeletal muscle tissue, the expression of miR-486-3p is significantly lower than that of miR-486-5p and is not affected by the SNP genotype. These findings further support the notion that miR-486-5p represents the predominantly active strand in skeletal muscle.

Accordingly, we hypothesized that the association between the C/C genotype and T2D susceptibility could be explained by the concurrent overexpression of sAnk1 and miR-486-5p due to the increased activity of the P2 promoter. To test this, we crossed transgenic mice overexpressing sAnk1.5 with transgenic mice overexpressing miR-486. In the resulting D-Tg mice, levels of mmu-miR-486-5p in skeletal muscles were 3- to 10-fold higher than in WT mice; the levels of sAnk1.5 mRNA varied between 3 and 30 folds higher compared to WT [31,57,58].

Of notice, in D-Tg mice, despite the high levels of sAnk1.5 mRNA, the sAnk1.5 protein levels were only increased between 0.3 and 0.5-fold compared to WT mice. Interestingly, a discrepancy between sAnk1.5 transcript and protein levels can also be observed in human skeletal muscle from C/C individuals, although this difference is less pronounced than that observed in D-Tg mice. Results from experiments performed with the proteasome inhibitor MG132, suggest that this discrepancy might be due to a ubiquitin-mediated post-translational regulation of sAnk1.5 expression, as previously observed in vivo in obscurin KO mice, and in vitro in non-muscular cells [15,51]. This evidence suggests that sAnk1.5 protein levels are regulated post-translationally to prevent protein accumulation, while still allowing independent modulation of miR-486 levels in physiological contexts where miR-486 may need to be upregulated, such as during myoblast differentiation, muscle growth, and physical exercise [33,34,43,59]. Indeed, examples of differential regulation between the levels of a given protein and those of microRNAs located within an intronic region of the same gene have been previously reported [60–63].

However, despite the observed increased expression of sAnk1.5 and miR-486-5p, a careful characterization of D-Tg mice revealed no differences in glucose handling or in alterations in other parameters associated with diabetic or pre-diabetic conditions, compared to WT animals. Specifically, no differences in body weight, muscle mass, or fat composition were observed between D-Tg mice and WT mice at any time point up to 12 months of age. Furthermore, responses to IPGTT, IPITT, blood insulin levels after glucose injection, and blood glucose levels after insulin injections did not differ between D-Tg and age-matched WT control mice.

Given that the GWAS data suggested only an association with

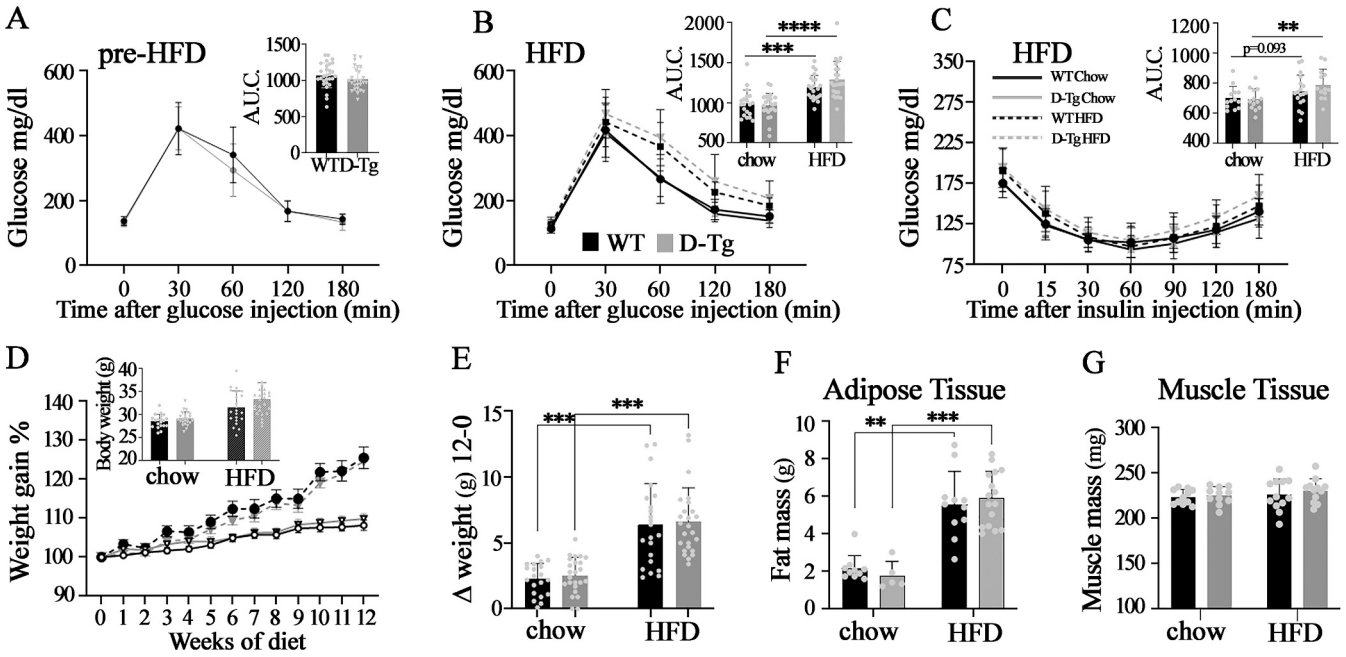

Fig. 6. HFD treatment in D-Tg mice. A. Glycemic curves and relative A.U.C. (inset) of IPGTT performed on 29 and 27 2-months-old WT and D-Tg mice, respectively, before starting the HFD treatment. These mice, and additional 33 animals from both genotypes, were divided into four groups and fed either standard diet (chow) or high fat diet (HFD) for twelve weeks (n = 20 WT-SD, 23 D-Tg-SD, 22 WT-HFD, 24 D-Tg-HFD). B. Glycemic curves and relative A.U.C. (inset) of IPGTT performed on WT and D-Tg mice at the end of the HFD period. C. Glycemic curves and relative A.U.C. (inset) of IPITT performed on WT and D-Tg mice at the end of the HFD period. D. Weekly weight gain recorded during the 12 weeks of treatment with HFD. Weight gain is expressed as a percentage ± sd relative to the beginning of the dietary regimen (week 0), which was set as 100 %. Average absolute body weight ± sd of the four experimental groups at the end of the treatment is reported in the inset. E. Increase in body weight (grams ± sd) of WT and D-Tg mice at the end of 12 weeks on a standard diet (chow) or HFD. F. Fat mass (grams ± sd) of WT and D-Tg mice at the end of 12 weeks on a standard diet (chow) or HFD (chow: n = 10 WT and 5 D-Tg; HFD: n = 11 WT and 16 D-Tg). G. Muscle mass (grams ± sd) of WT and D-Tg mice at the end of 12 weeks on a standard diet (chow) or HFD (chow: n = 11 WT and 11 D-Tg; HFD: n = 12 WT and 12 D-Tg). ** = $p < 0.01$, *** = $p < 0.001$, **** = $p < 0.0001$ as calculated by Two-way Anova. For all panels, bar colors and graph lines are as indicated in panels B and C, respectively.

Table 1
Absolute muscle weight in grams of wild type and D-Tg muscles under standard chow and HFD regimen.

Muscle weight (mg)	WT		D-Tg	
	Chow	HFD	Chow	HFD
TA	49,52 ± 4,06	49,06 ± 4,01	49,6 ± 1,58	50,07 ± 2,76
Gastro	153,3 ± 5,79	156,7 ± 12,4	155,4 ± 8,41	159,8 ± 10,2
EDL	11,46 ± 0,98	11,26 ± 1,15	11,20 ± 0,77	11,13 ± 0,70
Soleus	9,67 ± 0,81	9,17 ± 1,07	9,50 ± 0,66	9,78 ± 0,86

	Chow vs HFD *p-value WT*	Chow vs HFD *p-value D-Tg*	Chow vs D-Tg *p-value SC*	Chow vs D-Tg *p-value HFD*
TA	0,789	0,631	0,948	0,483
Gastro	0,421	0,267	0,520	0,506
EDL	0,652	0,832	0,485	0,744
Soleus	0,226	0,397	0,608	0,137

Upper panel: muscle weight of Tibialis anterior (TA), Gastrocnemius (Gastro), Extensor Digitorum Longus (EDL), and Soleus.
Lower panel: *p*-values of the different muscle weights under standard chow and HFD regimen.

susceptibility to T2D, we also tested the effect of exposing D-Tg mice to a high fat diet to promote the onset of a diabetic phenotype or reveal alterations in glucose metabolism [54,64]. However also following HFD treatment D-Tg mice did not present evident alterations in parameters associated with glucose metabolism.

In conclusion, the data presented here extend current knowledge on rs508419 as a functional SNP capable to modulate the expression levels of both sAnk1.5 and miR-486-5p in skeletal muscle tissue. Nevertheless, characterization of the glycemic profile in D-Tg mice, does not support the hypothesis that increased expression of sAnk1.5 and miR-486-5p might alter glucose homeostasis or contribute to T2D susceptibility in mice, at least under the reported experimental conditions. In fact, it is possible that increased age and/or additional stress conditions might reveal some metabolic disorders in D-Tg mice. In addition, we cannot rule out that miR-486 may unexpectedly regulate the expression of some of the potential target genes differently in humans and mice. On the other hand, it cannot be excluded an effect of the rs508419 SNP, beyond the upregulation of sAnk1.5 and miR-486 in C/C individuals.

Supplementary data to this article can be found online at https://doi.org/10.1016/j.bbamcr.2025.120087.

CRediT authorship contribution statement

S. Buonocore: Investigation, Formal analysis, Data curation. **F. Fiore:** Investigation, Formal analysis, Data curation. **E.M. Rubino:** Investigation, Data curation. **M.R. Catallo:** Investigation. **L. Raucci:** Investigation. **A. Laurino:** Writing – review & editing, Investigation, Data curation. **D. Rossi:** Writing – review & editing, Writing – original draft, Investigation, Formal analysis. **E. Pierantozzi:** Writing – review & editing, Writing – original draft, Investigation, Funding acquisition, Formal analysis, Conceptualization. **V. Sorrentino:** Writing – review & editing, Writing – original draft, Supervision, Funding acquisition, Formal analysis, Data curation, Conceptualization.

Declaration of competing interest

None.

Acknowledgements

This research was funded by grants to: E. Pierantozzi from Italian Ministry of Education, University and Research (MUR), PRIN2022, 20229A4WPC and V. Sorrentino from the Center for Gene Therapy and Drugs Based on RNA Technology, funded in the framework of the National Recovery and Resilience Plan (NRRP), M4C2 Inv, 1.4 CUP B63C22000610006 - Spoke 1" and from the Tuscany Health Ecosystem, funded in the framework of the National Recovery and Resilience Plan (NRRP), Missione 4 Componente 2 Inv. 1.5 CUP B63C22000680007 - Spoke 7". Both grants are, in turn, funded by the European Union-Next Generation EU.

Data availability

No data was used for the research described in the article.

References

[1] V. Bennett, A.J. Baines, Spectrin and ankyrin-based pathways: metazoan inventions for integrating cells into tissues, Physiol. Rev. 81 (3) (2001 Jul) 1353–1392, https://doi.org/10.1152/physrev.2001.81.3.1353.
[2] P.J. Mohler, V. Bennett, Defects in ankyrin-based cellular pathways in metazoan physiology, Front. Biosci. 1 (10) (2005 Sep) 2832–2840, https://doi.org/10.2741/1739.
[3] C.S. Birkenmeier, R.A. White, L.L. Peters, E.J. Hall, S.E. Lux, J.E. Barker, Complex patterns of sequence variation and multiple 5′ and 3′ ends are found among transcripts of the erythroid ankyrin gene, J. Biol. Chem. 268 (13) (1993 May 5) 9533–9540.
[4] P.G. Gallagher, W.T. Tse, A.L. Scarpa, S.E. Lux, B.G. Forget, Structure and organization of the human ankyrin-1 gene. Basis for complexity of pre-mRNA processing, J. Biol. Chem. 272 (31) (1997 Aug 1) 19220–19228, https://doi.org/10.1074/jbc.272.31.19220.
[5] D. Zhou, C.S. Birkenmeier, M.W. Williams, J.J. Sharp, J.E. Barker, R.J. Bloch, Small, membrane-bound, alternatively spliced forms of ankyrin 1 associated with the sarcoplasmic reticulum of mammalian skeletal muscle, J. Cell Biol. 136 (3) (1997 Feb 10) 621–631, https://doi.org/10.1083/jcb.136.3.621.
[6] P.G. Gallagher, B.G. Forget, An alternate promoter directs expression of a truncated, muscle-specific isoform of the human ankyrin 1 gene, J. Biol. Chem. 273 (3) (1998 Jan 16) 1339–1348, https://doi.org/10.1074/jbc.273.3.1339.
[7] C.S. Birkenmeier, J.J. Sharp, E.J. Gifford, S.A. Deveau, J.E. Barker, An alternative first exon in the distal end of the erythroid ankyrin gene leads to production of a small isoform containing an NH2-terminal membrane anchor, Genomics 50 (1) (1998 May 15) 79–88, https://doi.org/10.1006/geno.1998.5305.
[8] P. Young, E. Ehler, M. Gautel, Obscurin, a giant sarcomeric rho guanine nucleotide exchange factor protein involved in sarcomere assembly, J. Cell Biol. 154 (1) (2001 Jul 9) 123–136, https://doi.org/10.1083/jcb.200102110.
[9] M.L. Bang, T. Centner, F. Fornoff, A.J. Geach, M. Gotthardt, M. McNabb, C.C. Witt, D. Labeit, C.C. Gregorio, H. Granzier, S. Labeit, The complete gene sequence of titin, expression of an unusual approximately 700-kDa titin isoform, and its interaction with obscurin identify a novel Z-line to I-band linking system, Circ. Res. 89 (11) (2001 Nov 23) 1065–1072, https://doi.org/10.1161/hh2301.100981.
[10] D. Randazzo, E. Pierantozzi, D. Rossi, V. Sorrentino, The potential of obscurin as a therapeutic target in muscle disorders, Expert Opin. Ther. Targets 21 (9) (2017 Sep) 897–910, https://doi.org/10.1080/14728222.2017.1361931.
[11] P. Bagnato, V. Barone, E. Giacomello, D. Rossi, V. Sorrentino, Binding of an ankyrin-1 isoform to obscurin suggests a molecular link between the sarcoplasmic reticulum and myofibrils in striated muscles, J. Cell Biol. 160 (2) (2003 Jan 20) 245–253, https://doi.org/10.1083/jcb.200208109.
[12] A. Kontrogianni-Konstantopoulos, E.M. Jones, D.B. Van Rossum, R.J. Bloch, Obscurin is a ligand for small ankyrin 1 in skeletal muscle, Mol. Biol. Cell 14 (3) (2003 Mar) 1138–1148, https://doi.org/10.1091/mbc.e02-07-0411.
[13] A. Armani, S. Galli, E. Giacomello, P. Bagnato, V. Barone, D. Rossi, V. Sorrentino, Molecular interactions with obscurin are involved in the localization of muscle-specific small ankyrin1 isoforms to subcompartments of the sarcoplasmic reticulum, Exp. Cell Res. 312 (18) (2006 Nov 1) 3546–3558, https://doi.org/10.1016/j.yexcr.2006.07.027.
[14] M.A. Borzok, D.H. Catino, J.D. Nicholson, A. Kontrogianni-Konstantopoulos, R. J. Bloch, Mapping the binding site on small ankyrin 1 for obscurin, J. Biol. Chem. 282 (44) (2007 Nov 2) 32384–32396, https://doi.org/10.1074/jbc.M704089200.
[15] S. Lange, K. Ouyang, G. Meyer, L. Cui, H. Cheng, R.L. Lieber, J. Chen, Obscurin determines the architecture of the longitudinal sarcoplasmic reticulum, J. Cell Sci. 122 (Pt 15) (2009 Aug 1) 2640–2650, https://doi.org/10.1242/jcs.046193.
[16] B. Busby, T. Oashi, C.D. Willis, M.A. Ackermann, A. Kontrogianni-Konstantopoulos, A.D. Mackerell Jr., R.J. Bloch, Electrostatic interactions mediate binding of obscurin to small ankyrin 1: biochemical and molecular modeling studies, J. Mol. Biol. 408 (2) (2011 Apr 29) 321–334, https://doi.org/10.1016/j.jmb.2011.01.053.
[17] M.A. Ackermann, A.P. Ziman, J. Strong, Y. Zhang, A.K. Hartford, C.W. Ward, W. R. Randall, A. Kontrogianni-Konstantopoulos, R.J. Bloch, Integrity of the network sarcoplasmic reticulum in skeletal muscle requires small ankyrin 1, J. Cell Sci. 124 (Pt 21) (2011 Nov 1) 3619–3630, https://doi.org/10.1242/jcs.085159.
[18] E. Giacomello, M. Quarta, C. Paolini, R. Squecco, P. Fusco, L. Toniolo, B. Blaauw, L. Formoso, D. Rossi, C. Birkenmeier, L.L. Peters, F. Francini, F. Protasi, C. Reggiani, V. Sorrentino, Deletion of small ankyrin 1 (sAnk1) isoforms results in structural and functional alterations in aging skeletal muscle fibers, Am. J. Physiol. Cell Physiol. 308 (2) (2015 Jan 15) C123–C138, https://doi.org/10.1152/ajpcell.00090.2014.
[19] E. Pierantozzi, P. Szentesi, D. Al-Gaadi, T. Oláh, B. Dienes, M. Sztretye, D. Rossi, V. Sorrentino, L. Csernoch, Calcium homeostasis is modified in skeletal muscle fibers of small ankyrin1 knockout mice, Int. J. Mol. Sci. 20 (13) (2019 Jul 9) 3361, https://doi.org/10.3390/ijms20133361.
[20] F. Protasi, B. Girolami, S. Roccabianca, D. Rossi, Store-operated calcium entry: from physiology to tubular aggregate myopathy, Curr. Opin. Pharmacol. 68 (2023 Feb) 102347, https://doi.org/10.1016/j.coph.2022.102347.
[21] R. Rizzuto, T. Pozzan, Microdomains of intracellular Ca2+: molecular determinants and functional consequences, Physiol. Rev. 86 (1) (2006 Jan) 369–408, https://doi.org/10.1152/physrev.00004.2005.
[22] P.F. Desmond, J. Muriel, M.L. Markwardt, M.A. Rizzo, R.J. Bloch, Identification of small ankyrin 1 as a novel sarco(endo)plasmic reticulum Ca2+-ATPase 1 (SERCA1) regulatory protein in skeletal muscle, J. Biol. Chem. 290 (46) (2015 Nov 13) 27854–27867, https://doi.org/10.1074/jbc.M115.676585.
[23] P.F. Desmond, A. Labuza, J. Muriel, M.L. Markwardt, A.E. Mancini, M.A. Rizzo, R. J. Bloch, Interactions between small ankyrin 1 and sarcolipin coordinately regulate activity of the sarco(endo)plasmic reticulum Ca2+-ATPase (SERCA1), J. Biol. Chem. 292 (26) (2017 Jun 30) 10961–10972, https://doi.org/10.1074/jbc.M117.783613.
[24] Y. Li, N.T. Wright, R.J. Bloch, The juxtamembrane sequence of small ankyrin 1 mediates the binding of its cytoplasmic domain to SERCA1 and is required for inhibitory activity, J. Biol. Chem. 301 (3) (2025 Mar) 108216, https://doi.org/10.1016/j.jbc.2025.108216.
[25] R. Yan, S. Lai, Y. Yang, H. Shi, Z. Cai, V. Sorrentino, H. Du, H. Chen, A novel type 2 diabetes risk allele increases the promoter activity of the muscle-specific small ankyrin 1 gene, Sci. Rep. 6 (2016 Apr 28) 25105, https://doi.org/10.1038/srep25105.
[26] L.J. Scott, M.R. Erdos, J.R. Huyghe, R.P. Welch, A.T. Beck, B.N. Wolford, P. S. Chines, J.P. Didion, N. Narisu, H.M. Stringham, D.L. Taylor, A.U. Jackson, S. Vadlamudi, L.L. Bonnycastle, L. Kinnunen, J. Saramies, J. Sundvall, R. D. Albanus, A. Kiseleva, J. Hensley, G.E. Crawford, H. Jiang, X. Wen, R. M. Watanabe, T.A. Lakka, K.L. Mohlke, M. Laakso, J. Tuomilehto, H.A. Koistinen, M. Boehnke, F.S. Collins, S.C. Parker, The genetic regulatory signature of type 2 diabetes in human skeletal muscle, Nat. Commun. 29 (7) (2016 Jun) 11764, https://doi.org/10.1038/ncomms11764.
[27] L. Sun, X. Zhang, T. Wang, M. Chen, H. Qiao, Association of ANK1 variants with new-onset type 2 diabetes in a Han Chinese population from northeast China, Exp. Ther. Med. 14 (4) (2017 Oct) 3184–3190, https://doi.org/10.3892/etm.2017.4866.
[28] N. Soranzo, S. Sanna, E. Wheeler, C. Gieger, D. Radke, J. Dupuis, N. Bouatia-Naji, C. Langenberg, I. Prokopenko, E. Stolerman, et al., Common variants at 10 genomic loci influence hemoglobin A_1(C) levels via glycemic and nonglycemic pathways, Diabetes 59 (12) (2010 Dec) 3229–3239, https://doi.org/10.2337/db10-0502.
[29] M. Imamura, S. Maeda, T. Yamauchi, K. Hara, K. Yasuda, T. Morizono, A. Takahashi, M. Horikoshi, M. Nakamura, H. Fujita, et al., A single-nucleotide polymorphism in ANK1 is associated with susceptibility to type 2 diabetes in Japanese populations, Hum. Mol. Genet. 21 (13) (2012 Jul 1) 3042–3049, https://doi.org/10.1093/hmg/dds113.
[30] M.N. Harder, R. Ribel-Madsen, J.M. Justesen, T. Sparsø, E.A. Andersson, N. Grarup, T. Jørgensen, A. Linneberg, T. Hansen, O. Pedersen, Type 2 diabetes risk alleles near BCAR1 and in ANK1 associate with decreased β-cell function whereas risk alleles near ANKRD55 and GRB14 associate with decreased insulin sensitivity in the Danish Inter99 cohort, J. Clin. Endocrinol. Metab. 98 (4) (2013 Apr) E801–E806, https://doi.org/10.1210/jc.2012-4169.
[31] E. Pierantozzi, L. Raucci, S. Buonocore, E.M. Rubino, Q. Ding, A. Laurino, F. Fiore, M. Soldaini, J. Chen, D. Rossi, P. Vangheluwe, H. Chen, V. Sorrentino, Skeletal muscle overexpression of sAnk1.5 in transgenic mice does not predispose to type 2 diabetes, Sci. Rep. 13 (1) (2023 May 20) 8195, https://doi.org/10.1038/s41598-023-35393-0.
[32] E.M. Small, J.R. O'Rourke, V. Moresi, L.B. Sutherland, J. McAnally, R.D. Gerard, J. A. Richardson, E.N. Olson, Regulation of PI3-kinase/Akt signaling by muscle-enriched microRNA-486, Proc. Natl. Acad. Sci. U. S. A. 107 (9) (2010 Mar 2) 4218–4223, https://doi.org/10.1073/pnas.1000300107.
[33] B.K. Dey, J. Gagan, A. Dutta, miR-206 and -486 induce myoblast differentiation by downregulating Pax7, Mol. Cell. Biol. 31 (1) (2011) 203–214.
[34] M.S. Alexander, J.C. Casar, N. Motohashi, N.M. Vieira, I. Eisenberg, J.L. Marshall, M.J. Gasperini, A. Lek, J.A. Myers, E.A. Estrella, P.B. Kang, F. Shapiro, F. Rahimov, G. Kawahara, J.J. Widrick, L.M. Kunkel, MicroRNA-486-dependent modulation of DOCK3/PTEN/AKT signaling pathways improves muscular dystrophy-associated symptoms, J. Clin. Invest. 124 (6) (2014 Jun) 2651–2667, https://doi.org/10.1172/JCI73579.
[35] K. Hitachi, M. Nakatani, K. Tsuchida, Myostatin signaling regulates Akt activity via the regulation of miR-486 expression, Int. J. Biochem. Cell Biol. 47 (2014 Feb) 93–103, https://doi.org/10.1016/j.biocel.2013.12.003.
[36] H.H. Zhu, X.T. Wang, Y.H. Sun, W.K. He, J.B. Liang, B.H. Mo, L. Li, Microrna-486-5p targeting PTEN protects against coronary microembolization-induced cardiomyocyte apoptosis in rats by activating the PI3K/AKT pathway, Eur. J.

Pharmacol. 855 (15) (2019 Jul) 244–251, https://doi.org/10.1016/j.ejphar.2019.03.045.
[37] A. Douvris, J. Viñas, K.D. Burns, miRNA-486-5p: signaling targets and role in non-malignant disease, Cell. Mol. Life Sci. 79 (7) (2022 Jun 22) 376, https://doi.org/10.1007/s00018-022-04406-y.
[38] M.S. Alexander, J.C. Casar, N. Motohashi, J.A. Myers, I. Eisenberg, R.T. Gonzalez, E.A. Estrella, P.B. Kang, G. Kawahara, L.M. Kunkel, Regulation of DMD pathology by an ankyrin-encoded miRNA, Skelet. Muscle 8 (1) (2011 Aug) 27, https://doi.org/10.1186/2044-5040-1-27.
[39] Y. Peng, Y. Dai, C. Hitchcock, X. Yang, E.S. Kassis, L. Liu, Z. Luo, H.L. Sun, R. Cui, H. Wei, T. Kim, T.J. Lee, Y.J. Jeon, G.J. Nuovo, S. Volinia, Q. He, J. Yu, P. Nana-Sinkam, C.M. Croce, Insulin growth factor signaling is regulated by microRNA-486, an underexpressed microRNA in lung cancer, Proc. Natl. Acad. Sci. U. S. A. 110 (37) (2013 Sep 10) 15043–15048, https://doi.org/10.1073/pnas.1307107110.
[40] R.A. Youness, M.A. Rahmoon, R.A. Assal, A.I. Gomaa, M.T. Hamza, I. Waked, H. M. El Tayebi, A.I. Abdelaziz, Contradicting interplay between insulin-like growth factor-1 and miR-486-5p in primary NK cells and hepatoma cell lines with a contemporary inhibitory impact on HCC tumor progression, Growth Factors 34 (3–4) (2016 Aug) 128–140, https://doi.org/10.1080/08977194.2016.1200571.
[41] R. Wang, B. Kumar, E.H. Doud, A.L. Mosley, M.S. Alexander, L.M. Kunkel, H. Nakshatri, Skeletal muscle-specific overexpression of miR-486 limits mammary tumor-induced skeletal muscle functional limitations, Mol. Ther. Nucleic Acids 28 (2022 Mar 16) 231–248, https://doi.org/10.1016/j.omtn.2022.03.009. Erratum in: Mol Ther Nucleic Acids. 2022 Aug 20;29:614–616. doi: https://doi.org/10.1016/j.omtn.2022.08.022.
[42] A. Samani, R.M. Hightower, A.L. Reid, K.G. English, M.A. Lopez, J.S. Doyle, M. J. Conklin, D.A. Schneider, M.M. Bamman, J.J. Widrick, D.K. Crossman, M. Xie, D. Jee, E.C. Lai, M.S. Alexander, miR-486 is essential for muscle function and suppresses a dystrophic transcriptome, Life Sci. Alliance. 5 (9) (2022 May 5) e202101215, https://doi.org/10.26508/lsa.202101215.
[43] W. Jung, U. Juang, S. Gwon, H. Nguyen, Q. Huang, S. Lee, B. Lee, S.H. Kwon, S. H. Kim, J. Park, Microrna-mediated regulation of muscular atrophy: exploring molecular pathways and therapeutics (review), Mol. Med. Rep. 29 (6) (2024 Jun) 98, https://doi.org/10.3892/mmr.2024.13222.
[44] D. Rossi, L. Gigli, A. Gamberucci, R. Bordoni, A. Pietrelli, S. Lorenzini, E. Pierantozzi, G. Peretto, G. De Bellis, P. Della Bella, M. Ferrari, V. Sorrentino, S. Benedetti, S. Sala, C. Di Resta, A novel homozygous mutation in the TRDN gene causes a severe form of pediatric malignant ventricular arrhythmia, Heart Rhythm 17 (2) (2020 Feb) 296–304, https://doi.org/10.1016/j.hrthm.2019.08.018.
[45] D. Rossi, J. Palmio, A. Evilä, L. Galli, V. Barone, T.A. Caldwell, R.A. Policke, E. Aldkheil, C.E. Berndsen, N.T. Wright, E. Malfatti, G. Brochier, E. Pierantozzi, A. Jordanova, V. Guergueltcheva, N.B. Romero, P. Hackman, B. Eymard, B. Udd, V. Sorrentino, A novel FLNC frameshift and an OBSCN variant in a family with distal muscular dystrophy, PloS One 12 (10) (2017 Oct 26) e0186642, https://doi.org/10.1371/journal.pone.0186642.
[46] V. Barone, E. Mazzoli, J. Kunic, D. Rossi, S. Tronnolone, V. Sorrentino, Yip1B isoform is localized at ER-Golgi intermediate and cis-Golgi compartments and is not required for maintenance of the Golgi structure in skeletal muscle, Histochem. Cell Biol. 143 (3) (2015 Mar) 235–243, https://doi.org/10.1007/s00418-014-1277-z.
[47] M.W. Pfaffl, A new mathematical model for relative quantification in real-time RT-PCR, Nucleic Acids Res. 29 (9) (2001 May 1) e45, https://doi.org/10.1093/nar/29.9.e45.
[48] J.M. Pioner, E. Pierantozzi, R. Coppini, E.M. Rubino, V. Biasci, G. Vitale, A. Laurino, L. Santini, M. Scardigli, D. Randazzo, et al., Obscurin deficiency leads to compensated dilated cardiomyopathy and increased arrhythmias, J. Gen. Physiol. 157 (4) (2025 Jul 7) e202413696, https://doi.org/10.1085/jgp.202413696.
[49] D. Randazzo, E. Giacomello, S. Lorenzini, D. Rossi, E. Pierantozzi, B. Blaauw, C. Reggiani, S. Lange, A.K. Peter, J. Chen, V. Sorrentino, Obscurin is required for ankyrinB-dependent dystrophin localization and sarcolemma integrity, J. Cell Biol. 200 (4) (2013 Feb 18) 523–536, https://doi.org/10.1083/jcb.201205118.
[50] G.N.A. Vattemi, D. Rossi, L. Galli, M.R. Catallo, E. Pancheri, G. Marchetto, B. Cisterna, M. Malatesta, E. Pierantozzi, P. Tonin, V. Sorrentino, Ryanodine receptor 1 (RYR1) mutations in two patients with tubular aggregate myopathy, Eur. J. Neurosci. 56 (3) (2022 Aug) 4214–4223, https://doi.org/10.1111/ejn.15728.
[51] S. Lange, S. Perera, P. Teh, J. Chen, Obscurin and KCTD6 regulate cullin-dependent small ankyrin-1 (sAnk1.5) protein turnover, Mol. Biol. Cell 23 (13) (2012 Jul) 2490–2504, https://doi.org/10.1091/mbc.E12-01-0052.
[52] N.T. Seyfried, P. Xu, D.M. Duong, D. Cheng, J. Hanfelt, J. Peng, Systematic approach for validating the ubiquitinated proteome, Anal. Chem. 80 (11) (2008 Jun 1) 4161–4169, https://doi.org/10.1021/ac702516a.
[53] X. Huang, G. Liu, J. Guo, Z. Su, The PI3K/AKT pathway in obesity and type 2 diabetes, Int. J. Biol. Sci. 14 (11) (2018 Aug 6) 1483–1496, https://doi.org/10.7150/ijbs.27173.
[54] R.J. Fajardo, L. Karim, V.I. Calley, M.L. Bouxsein, A review of rodent models of type 2 diabetic skeletal fragility, J. Bone Miner. Res. 29 (5) (2014) 1025–1040, https://doi.org/10.1002/jbmr.2210.
[55] J. Li, H. Wu, Y. Liu, L. Yang, High fat diet induced obesity model using four strains of mice: Kunming, C57BL/6, BALB/c and ICR, Exp. Anim. 69 (3) (2020 Aug 5) 326–335, https://doi.org/10.1538/expanim.19-0148.
[56] A.M. El Khouly, R.A. Youness, M.Z. Gad, Microrna-486-5p and microrna-486-3p: multifaceted pleiotropic mediators in oncological and non-oncological conditions, Noncoding RNA Res. 5 (1) (2020 Jan 9) 11–21, https://doi.org/10.1016/j.ncrna.2020.01.001.
[57] A. Musarò, K. McCullagh, A. Paul, L. Houghton, G. Dobrowolny, M. Molinaro, E. R. Barton, H.L. Sweeney, N. Rosenthal, Localized Igf-1 transgene expression sustains hypertrophy and regeneration in senescent skeletal muscle, Nat. Genet. 27 (2) (2001 Feb) 195–200, https://doi.org/10.1038/84839.
[58] P.S. Zammit, A. Cohen, M.E. Buckingham, R.G. Kelly, Integration of embryonic and fetal skeletal myogenic programs at the myosin light chain 1f/3f locus, Dev. Biol. 313 (1) (2008 Jan 1) 420–433, https://doi.org/10.1016/j.ydbio.2007.10.044.
[59] H.E. Gao, F.H. Li, T. Xie, S. Ma, Y.B. Qiao, D.S. Wu, L. Sun, Lifelong exercise in age rats improves skeletal muscle function and MicroRNA profile, Med. Sci. Sports Exerc. 53 (9) (2021 Sep 1) 1873–1882, https://doi.org/10.1249/MSS.0000000000002661.
[60] N. Ma, X. Wang, Y. Qiao, F. Li, Y. Hui, C. Zou, J. Jin, G. Lv, Y. Peng, L. Wang, H. Huang, L. Zhou, X. Zheng, X. Gao, Coexpression of an intronic microRNA and its host gene reveals a potential role for miR-483-5p as an IGF2 partner, Mol. Cell. Endocrinol. 333 (1) (2011 Feb 10) 96–101, https://doi.org/10.1016/j.mce.2010.11.027.
[61] C. van Solingen, L. Seghers, R. Bijkerk, J.M. Duijs, M.K. Roeten, A.M. van Oeveren-Rietdijk, H.J. Baelde, M. Monge, J.B. Vos, H.C. de Boer, P.H. Quax, T.J. Rabelink, A.J. van Zonneveld, Antagomir-mediated silencing of endothelial cell specific microRNA-126 impairs ischemia-induced angiogenesis, J. Cell. Mol. Med. 13 (8A) (2009 Aug) 1577–1585, https://doi.org/10.1111/j.1582-4934.2008.00613.x.
[62] S. Quah, P.W. Holland, The Hox cluster microRNA miR-615: a case study of intronic microRNA evolution, Evodevo 6 (2015 Oct 7) 31, https://doi.org/10.1186/s13227-015-0027-1.
[63] S. Barik, An intronic microRNA silences genes that are functionally antagonistic to its host gene, Nucleic Acids Res. 36 (16) (2008 Sep) 5232–5241, https://doi.org/10.1093/nar/gkn513.
[64] R. Buettner, J. Schölmerich, L.C. Bollheimer, High-fat diets: modeling the metabolic disorders of human obesity in rodents, Obesity (Silver Spring) 15 (4) (2007 Apr) 798–808, https://doi.org/10.1038/oby.2007.608.